THE JOURNAL OF BIOLOGICAL CHEMISTRY
Vol. 252, No. 7, Issue of April 10, pp. 2331-2337, 1977
Printed in U.S.A.

Oxygen Equilibrium Curve of Normal Human Blood and Its Evaluation by Adair's Equation

(Received for publication, December 2, 1976)

ROBERT M. WINSLOW AND MEI-LIE SWENBERG

From the Molecular Hematology Branch, National Heart and Lung Institute, National Institutes of Health, Bethesda, Maryland 20014

ROBERT L. BERGER

From the Laboratory of Technical Development, National Heart and Lung Institute, National Institutes of Health, Bethesda, Maryland 20014

RICHARD I. SHRAGER

From the Laboratory of Statistical and Mathematical Methodology, Division of Computer Research and Technology, National Institutes of Health, Bethesda, Maryland 20014

MASSIMO LUZZANA, MICHELE SAMAJA, AND LUIGI ROSSI-BERNARDI

From the Cattedra di Enzimologia, University of Milan, Milan, Italy 20133

Oxygen equilibrium curves of fresh, normal human blood have been measured by new methods which allow the control of pH, p_{CO_2}, and 2,3-diphosphoglycerate and which yield higher accuracy at the extremes of saturation than was possible previously. The curve determined by these techniques lies slightly to the right of the standard curve of Roughton *et al.* (Roughton, F. J. W., Deland, E. C., Kernohan, J. C., and Severinghaus, J. W. (1972) in *Oxygen Affinity of Hemoglobin and Red Cell Acid Base Status* (Astrup, P., and Rørth, M., eds) pp. 73-83, Academic Press, New York). The greatest difference is at low oxygen saturation, probably owing to the fact that the latter data were obtained under conditions which would lead to depletion of cellular 2,3-diphosphoglycerate. The range of p_{50} (oxygen pressure at half-saturation) values for four normal subjects was 28.3 mm Hg to 29.0 mm Hg.

Adair's stepwise oxygenation scheme has been used to analyze the curves with the result that $a_1 = 0.1514 \times 10^{-1}$ (± 10%) mm^{-1}; $a_2 = 0.9723 \times 10^{-3}$ (± 8%) mm^{-2}; $a_3 = 0.1703 \times 10^{-3}$ (± 50%) mm^{-3}; $a_4 = 0.1671 \times 10^{-5}$ (± 2%) mm^{-4} for the best of four data sets. Because these constants are very sensitive to changes in the shape of the oxygenation curve, this analysis is much more useful than p_{50} measurements in the investigation of the various allosteric effectors of the function of hemoglobin within the red cell.

Although a number of theoretical questions remain in regard to the details of hemoglobin-oxygen interactions, a reasonably clear overall picture can be presented (for example, see Ref. 1). This understanding is possible because of parallel studies of the functional and structural properties of hemoglobin solutions and have led to a description of the influence of various effectors (principally 2,3-diphosphoglycerate, H^+, and CO_2) on the equilibrium and kinetic reactions. A major contribution to this field has been the development of methods for the precise measurement of the hemoglobin-oxygen equilibrium curve, especially at extremely high and low oxygen saturation (2). In particular, evaluation of equilibrium data in terms of the generalized Adair equation (3) allowed Imai and co-workers to quantitate the effects of H^+, 2,3-DPG,[1] and temperature, and to compare the properties of various hemoglobin derivatives (4-7). The principal value of the Adair analysis is that it is sensitive to changes in the shape of the oxygen equilibrium curve.

Whole blood is a far more complex system than is hemoglobin in solution, and to date, most investigations into the regulation of the blood oxygen equilibrium curve have dealt with p_{50} values, measures of the position of the curve. Quantitation of the roles of the various allosteric effectors in whole blood has been retarded because of a lack of methods by which the precise whole blood oxygen equilibrium curve could be obtained. Roughton *et al.* (8) evaluated the blood oxygen equilibrium data according to Adair's generalized formula (3):

$$Y = \frac{a_1p + a_2p^2 + a_3p^3 + a_4p^4}{4(1 + a_1p + a_2p^2 + a_3p^3 + a_4p^4)} \quad (1)$$

where Y is fractional saturation and p, oxygen pressure. The experiments, however, were performed before the importance of 2,3-DPG was fully appreciated and their methods were so laborious that preservation of this compound was impossible.

[1] The abbreviations used are: 2,3-DPG, 2,3-diphosphoglycerate; Hb, hemoglobin; MetHb, methemoglobin; COHb, carboxyhemoglobin.

In order to investigate the *in vivo* regulation of hemoglobin oxygen affinity in normal red cells and in pathological states, we have sought a method which would yield data of precision equal to that possible for pure hemoglobin. The method described by Rossi-Bernardi, *et al.* (9) allows strict control of pH and p_{CO_2} during the measurement and can be done quickly enough so that 2,3-DPG concentration is maintained. We have previously described its application in the study of blood from subjects with sickle cell disease and some of its shortcomings (10). Although it is quite reliable in the middle range of saturation, it does not yield data of sufficient precision at extremes of oxygenation to permit analysis in terms of the Adair equation. Therefore, a mixing method has been employed to explore these critical regions of saturation. We present here the method and the results of our analysis of oxygen equilibrium curves for normal, fresh human blood.

EXPERIMENTAL PROCEDURES

Hematological Measurements—All blood samples were drawn less than 2 h (and usually less than 20 min) before their use. The blood was mixed with heparin (100 units/ml) and immediately chilled to 4°. Measurement of Hb, MetHb, and COHb was by a modification of the method of Rossi-Bernardi *et al.* (11). Well mixed, whole blood (10 μl) was mixed with 1.0 ml of a Sterox/borate solution (10 mM $Na_2B_4O_7$, 0.01% (v/v) Sterox, pH 9.14). The optical density was measured at 497, 565, and 620 nm with a Cary 118C spectrophotometer (Varian). Using the extinction coefficients for oxyhemoglobin, methemoglobin, and CO-hemoglobin at these wavelengths (11), their relative concentrations were determined. 2,3-DPG was measured according to Nygaard and Rørth (12) using kits from Sigma.

Calibration of Oxygen Electrode—The oxygen electrode (model 20335, Instrumentation Laboratories, Lexington, Mass.) was mounted in the apparatus described previously (9). It was fitted with Teflon membrane 5937, from Yellow Springs Instruments, Yellow Springs, Ohio, for p_{O_2} less than 150 mm Hg, and polypropylene membrane (19010 Instrumentation Laboratories) for p_{O_2} above 150 mm Hg. The electrolyte was a modification of that described by Hahn *et al.* (13). It contained 1.0 M KH_2PO_4, 0.1 M NaCl and was titrated to pH 10.2 with solid NaOH.

Gas mixtures were obtained from Lifogen Inc. (Cambridge, Md.) and their compositions were certified nominally to ±0.02%. The gases were humidified at 37° and then directed into the chamber of the reaction cuvette. The output from the oxygen electrode was calibrated by equilibrating water with O_2(N_2 mixtures of varying compositon. Blood samples were equilibrated with selected gases in an IL model 237 tonometer (Instrumentation Laboratories, Lexington, Mass.) for 20 to 30 min each. The output from the electrode was then checked when the cuvette was flushed with equilibrating gas and the blood separately. The results of these procedures were used to determine the true p_{O_2} of blood.

Middle Oxygen Equilibrium Curve—The middle portion of the blood oxygen equilibrium curve was measured as described previously (10). Two milliliters of blood were deoxygenated for 30 min at 37° in an IL 237 tonometer in the presence of 5.6% CO_2 (balance N_2). During oxygenation of a 1-ml sample by the slow addition of hydrogen peroxide (Parke-Davis) in the presence of catalase (Sigma) p_{CO_2} was monitored with an IL 17026 CO_2 electrode fitted with a Teflon membrane (Beckman, 77948D). pH and p_{CO_2} were held constant by the addition of 0.4 M NaOH from a micrometer syringe. By this method, the p_{CO_2} could be maintained between ±0.2 mm Hg and pH between ±0.01 units. The total amount of NaOH required for this procedure was recorded.

Mixing Experiments—A sample of blood was divided into two portions, one of which was equilibrated with 94.4% N_2, balance CO_2. The second sample was subjected to a brief centrifugation to pack the red cells and 0.4 M NaOH was added to the separated plasma to bring the NaOH concentration up to that at the end of the H_2O_2 run. After equilibration of the plasma with 94.4% O_2 (balance CO_2) for 5 min, the red cells were added back and equilibration was continued. Both samples were equilibrated with their respective gases for a period of 30 min. A cuvette was loaded with 1 ml of oxygenated blood with a gas-tight syringe (Hamilton, Reno, Nev.). Deoxygenated blood was taken up in a 1-ml gas-tight syringe containing a small magnetic stirrer. The cells were kept in suspension by gently moving a magnet along the side of the syringe. Small aliquots (2 to 5 μl) were added to the oxygenated blood through a 26 gauge needle, using a micrometer syringe drive. After each addition the p_{O_2} decreased quickly and then plateaued at a new level. When the p_{O_2} was stable, the next increment was added.

To obtain the bottom end of the oxygen equilibrium curve, the procedure was reversed: small increments of oxygenated blood were added to the deoxygenated blood in the cuvette. Complete deoxygenation could be checked by the addition of a small amount of sodium dithionite to the blood after the experiment. The rate of mixing in the cuvette was critical. If the rate was too low, the p_{O_2} measurement was erroneously low, possibly due to stagnation of blood at the surface of the oxygen electrode. To avoid this difficulty, the stirring rate was optimized so that the p_{O_2} reading was maximal.

Solubility Coefficient, α—When the cuvette contains oxygenated blood and the blood being injected into it is completely deoxygenated, the relationship between total oxygen in the cuvette before and after injection is:

$$T_i V = T_{i-1}(V - \Delta V_i)$$

where T_{i-1} is total O_2 concentration before the ith injection, T_i is total O_2 concentration after the ith injection, V is the volume of the cuvette, and ΔV_i is the volume of the ith injection. For all i, T_i is related to α by:

$$T_i = (\alpha P_i/760) + C_c S_i$$
$$\text{(Total)} = \text{(dissolved)} + \text{(bound)}$$

Where P_i is the p_{O_2} after the ith injection, S_i is fractional saturation after the ith injection, and C_c is the O_2 capacity of Hb per unit volume in the cuvette.

The quantities T_{i-1} and T_i can be eliminated by substituting (dissolved) + (bound) for (total), yielding:

$$\alpha = \frac{760\, C_c[V(S_i - S_{i-1}) + S_{i-1}\Delta V_i]}{P_{i-1}(V - \Delta V_i) - P_i V}$$

At very high hemoglobin saturation, S_{i-1} and S_i are nearly equal, and S_{i-1} is nearly 1. Therefore, if ΔV_i is not chosen too small, α may be approximated from the relation:

$$\lim_{P\to\infty} \frac{760\, C_s \Delta V_i}{P_{i-1}(V - \Delta V_i)} = \alpha \qquad (2)$$

where C_s is the oxygen capacity of hemoglobin per unit volume of the syringe.

In fact, an entire curve of approximations to α can be generated, one point for each ΔV_i, and the apparent limit of that curve at large P can be used as the value of α.

Calculation of Saturation from Mixing Data—The general formula for the calculation of the hemoglobin saturation at the ith point is

$$S_i = \frac{T_i - D_i}{C_c} \qquad (3)$$

where S_i is saturation, T_i is the total oxygen content of the cuvette after the ith addition, and D_i is dissolved oxygen.

At the ith incremental addition of volume ΔV_i of blood from the syringe where the total oxygen content is $\Delta V_i\, T_s$, an equal volume of blood with total oxygen content $\Delta V_i\, T_{i-1}$ is expelled. Mixing then occurs and the new total oxygen content is $V\, T_i$. This is given by

$$T_i = \frac{VT_{i-1} + \Delta V_i(T_s - T_{i-1})}{V}$$

or

$$T_i = T_s + (T_{i-1} - T_s)(1 - V_i/V) \qquad (4)$$

Thus, total oxygen concentration is given by Formula 4, dissolved oxygen concentration by (αP/760) and saturation by Formula 3. These equations apply to either the high or low saturation mixing experiments.

Complete Oxygen Equilibrium Curve—Since the error in the H_2O_2 curve is least at low saturation, it was always in close agreement with bottom mixing data. However, as described earlier (10), there is uncertainty in determination of the end point of the H_2O_2 saturation curve. To account for this uncertainty, the saturation at 100 mm was determined for each set of data by linear interpolation, and the ratio saturation (100 mm, top data)/saturation (100 mm, middle data) was

TABLE I

Clinical parameters of normal blood samples

	Subject[a]				
	RW	MS	FA	SC	Roughton *et al.* (8)
Hb (g/100 ml)	15.0	17.2	17.0	14.9	
Hematocrit (%)	43.0	46.5	44.5	44.3	
2,3-DPG[b]	0.89	0.78	0.92	0.95	
pH	7.42	7.42	7.42	7.42	7.4
p_{CO_2} (mm Hg)	40	40	40	40	40
p_{50} (mm Hg)	29.0	28.8	29.0	28.3	26.5
n_{max}[c]	2.6	2.6	2.5	2.7	2.7

[a] All subjects were males.

[b] Micromoles per μmol of hemoglobin tetramer. Normal range, 0.88 ± 0.08 (S.D.).

[c] Maximum slope of Hill plot.

used to adjust the middle data points. The value 100 mm was chosen somewhat arbitrarily; any point which was contained in both the high and middle saturation curves could be used. The complete curve was then obtained by joining the top, middle, and bottom portions and was subjected to the procedure for the determination of Adair's constants described under "Appendix."

All curve fitting was done on the MLAB system (14). This system uses the constrained nonlinear regression of Shrager (15, 16) which converges to a locally best solution with restrictions on the parameters. In this case the α's were required to be non-negative.

RESULTS

Hematologic Measurements – The subjects from which the blood for the present study was obtained were healthy, nonsmoking Caucasian males. Electrophoretic analysis revealed only the presence of Hemoglobins A and A_2. Hemoglobin concentration, hematocrit, and 2,3-DPG concentrations are given in Table I. The method used to measure hemoglobin, CO-hemoglobin and methemoglobin employs the spectrophotometric analysis at three wavelengths of blood which has been lysed, and diluted into Sterox/borate buffer, pH 9.14. Thus all hemoglobin is present as oxyhemoglobin, CO-hemoglobin, or methemoglobin. The oxygen capacity used to calculate saturation has taken into account the very small amounts of CO-hemoglobin and methemoglobin present.

Electrodes – The voltage output from the p_{O_2} electrode is linear with p_{O_2} up to 1 atm. The output in blood is somewhat less, and care must be taken to calibrate the electrode before precise work can be undertaken, especially at high p_{O_2}. In Fig. 1 the calibration of the electrode is described. The modified electrolyte described under "Experimental Procedures" gave a response (10 s, 90% response) which was much faster than that obtained with commercially available solutions (33010, IL or S-4064, Radiometer). Moreover, long "conditioning" periods in the appropriate p_{O_2} ranges to be used were not necessary.

The present experiments were performed at constant p_{CO_2} (40 mm Hg). In the case of the H_2O_2 curves, p_{CO_2} was held constant by titration of the H^+ liberated during oxygenation with NaOH. The response time of the CO_2 electrode was quite slow (54 s, 90% response). However, in unpublished control experiments, we have demonstrated that when the oxygenation time is greater than 10 min, the curve is identical to that obtained when H_2O_2 is added in steps with sufficient time allowed between steps for full equilibration of p_{CO_2}.

Mixing Experiments – A mixing experiment at high saturation is shown in Fig. 2. As saturation decreases larger aliquots of deoxygenated blood must be added in order to reduce p_{O_2} by a given amount. This is because at lower saturation a larger proportion of the O_2 taken up by the deoxygenated blood is

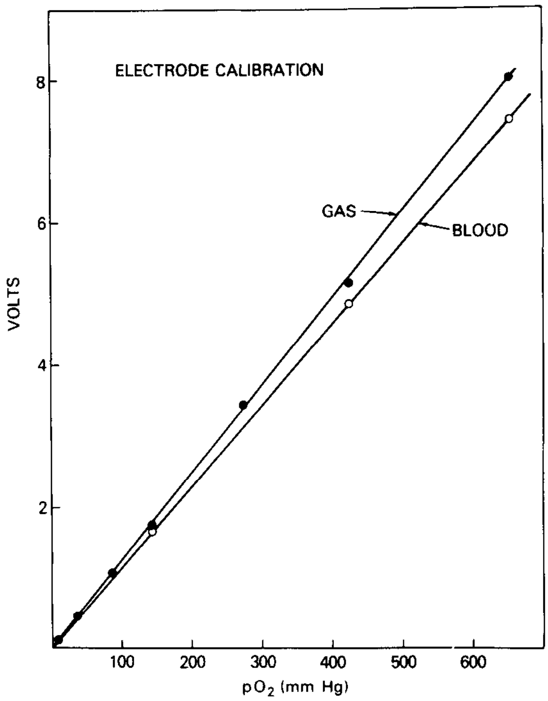

FIG. 1. Calibration of the oxygen electrode. The procedure is given under "Experimental Procedures." The response is linear, but the electrical output in blood is 95% of that in gas.

derived from hemoglobin, and a smaller proportion from solution (dissolved O_2 is measured by the oxygen electrode). Thus, when saturation is close to 100% the drop in p_{O_2} is nearly linear with the volume of deoxygenated blood added, and allows the estimate of the solubility coefficient α, described under "Experimental Procedures" (Fig. 2*B*).

An inherent difficulty in the method is that the assumption of 100% saturation of the oxygenated sample is required. The error introduced by this assumption however, is negligible because as discussed below, computer fit of the data to Adair's scheme does not improve appreciably by varying the saturation value of the oxygenated sample.

A low saturation mixing curve is shown in Fig. 3. It was essential to completely deoxygenate the sample and to calibrate the p_{O_2} electrode with low p_{O_2} gas (1% O_2). The zero point of the electrode must be checked at the end of the experiment by the addition of dithionite to the blood sample.

Solubility Coefficient, α – Roughton and co-workers used a similar method to evaluate the solubility coefficient (17). However, improved tonometry allows us to achieve higher p_{O_2} than was previously possible, so that unlike Roughton we estimate α at 37° for blood directly. Using our method, we find that α = 0.0234 ml/ml atm for normal human blood (range, 0.0230 to 0.0240 for four subjects) under standard conditions a value in good agreement with that reported by Roughton (0.0238). It must be pointed out that this analysis assumes that blood is a homogenous system and will not reflect possible differences between intracellular and extracellular solubility.

Middle Oxygen Equilibrium Curve – In addition to the solubility coefficient (α), hemoglobin concentration, and cuvette volume, the measurement of the oxygen equilibrium curve by the H_2O_2 method requires accurate knowledge of H_2O_2 concentration and its rate of addition. Since error can appear in these values, the data are subject to slightly greater uncertainty than are the mixing experiments. Although this causes little

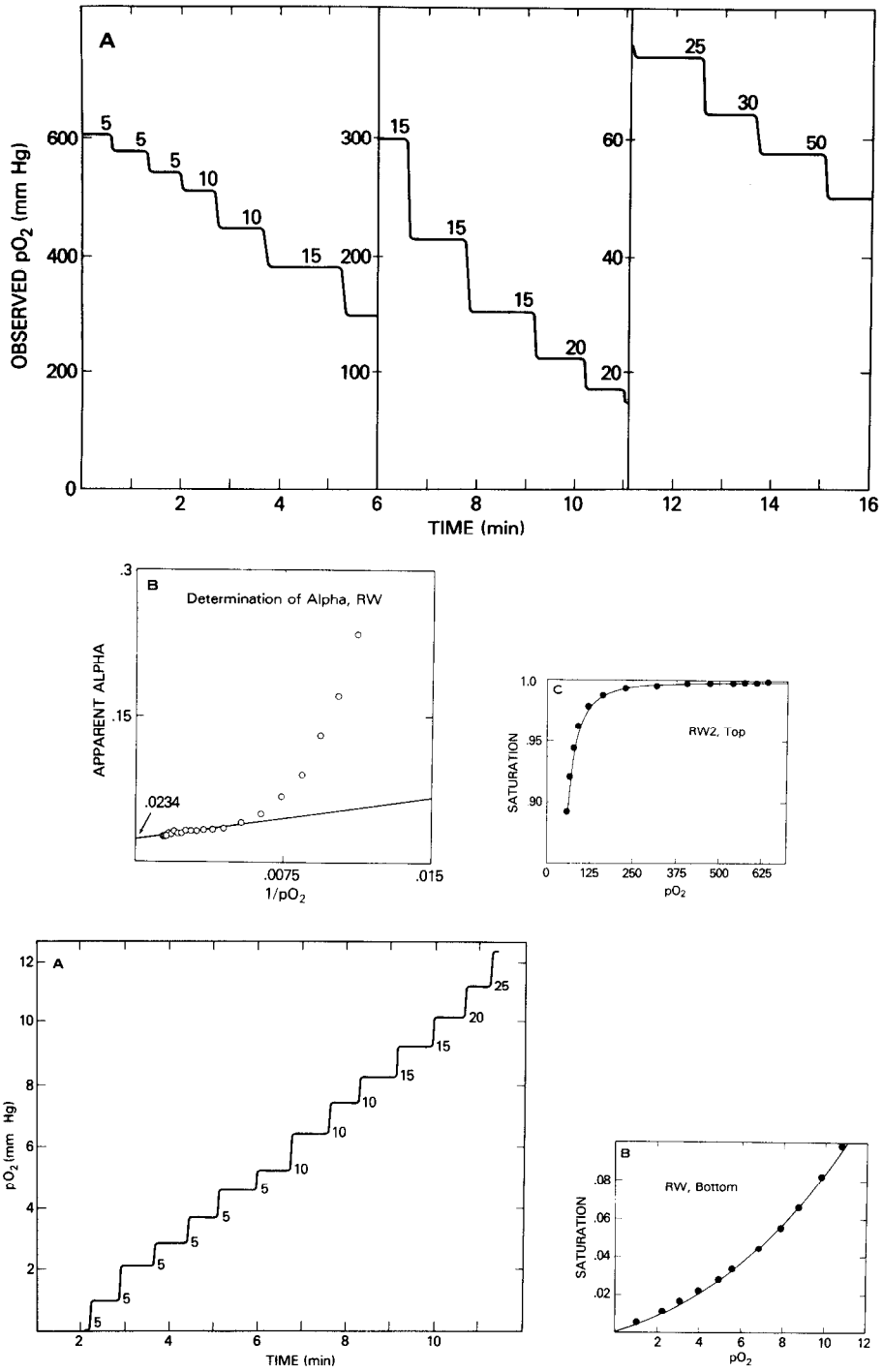

FIG. 2. The top of the blood oxygen equilibrium curve, obtained by the mixing method. The numbers in *A* represent the volumes of the small increments of deoxygenated blood which were added to the larger volume of oxygenated blood (1000 μl). In *B* the solubility coefficient, α, is estimated. As hemoglobin saturation approaches 100% the apparent α approaches a limiting value which is estimated by linear extrapolation to infinite p_{O_2} ($1/p_{O_2} = 0$). In this experiment, $\alpha = 0.0234$ ml/ml·atm. In *C* the final calculated data points are shown with the Adair curve obtained by fitting (see "Appendix").

FIG. 3. The bottom of the blood oxygen equilibrium curve obtained by the mixing method. The data were obtained by the reversal of the procedure outlined in Fig. 2. The raw data (*A*) were subjected to the analysis given under "Experimental Procedures" and the final calculated points are shown in *B* with the Adair curve.

error in the estimation of p_{50}, large uncertainty can be expected in the determination of the upper end of the curve. Thus, at 150 mm Hg, the end of the oxygenation run, saturation commonly ranges from 90 to 96%. One method of dealing with this problem by curve fitting has been described (10). Here, however, we assume that the blood samples in the middle and upper experiments achieve the same saturation at p_{O_2} of 100 mm Hg and a normalization is carried out as outlined under "Experimental Procedures." Minor variation in the saturation at 100 mm appears to be random, however, and Fig. 4 shows an example in which the data from each saturation range agree well without the normalization procedure. This result indicates that mismatching of high and low saturation mixing curves observed by others previously (18, 19) was due to experimental error, rather than to "hysteresis" in the oxygenation reaction.

The Complete Curve – In experiments with subject RW, saturation in the middle oxygen equilibrium curve was 96.44% at 100 mm Hg, while in the top end mixing curve it was 97.03%. Therefore, the middle oxygen equilibrium curve saturations were multiplied by 0.9703/0.9644 to obtain a final middle data set. No adjustments were required to match the bottom and middle data. The complete curve was then obtained by joining the bottom, middle, and top portions (Fig. 5, Table II).

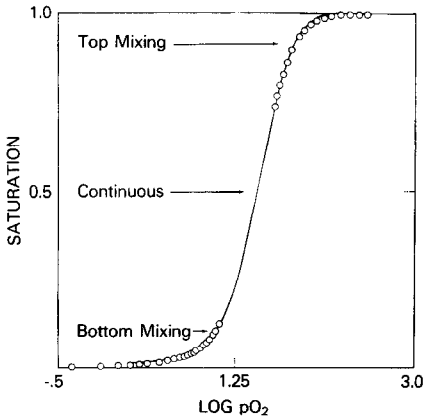

FIG. 4. Top, middle, and bottom portions of the oxygen equilibrium curve for subject MS. This figure demonstrates the extension of the curve which is possible by the mixing method: the continuous curve is least reliable at its extremes.

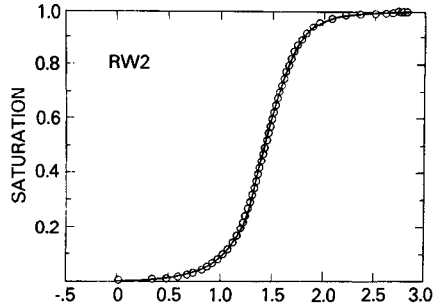

FIG. 5. The complete oxygen equilibrium curve for subject RW. Data for the three saturation ranges were joined and the resulting complete curve was subjected to the fitting procedure described under "Appendix." The data points (○) and the Adair fit (——) are shown.

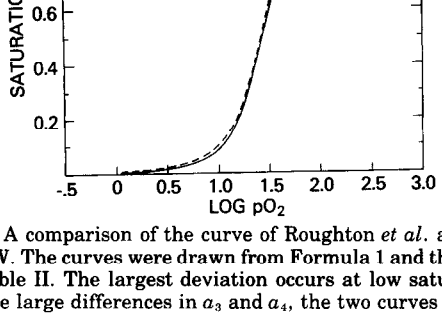

FIG. 6. A comparison of the curve of Roughton *et al.* and that of subject RW. The curves were drawn from Formula 1 and the parameters of Table II. The largest deviation occurs at low saturation. In spite of the large differences in a_3 and a_4, the two curves are nearly equivalent at high saturation.

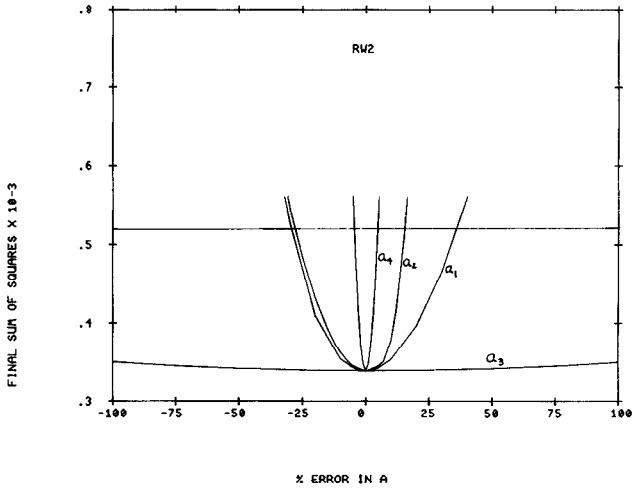

FIG. 7. Errors in Adair's parameters for data set RW2. The parameter a_i was systematially varied (*abscissa values*) and the other three a's were fit to the data set (Table II). The residual sum of squares from these fits are given on the *ordinate*. The 95% confidence limit (f test) is shown as a *horizontal line*.

TABLE II

RW2 data

p_{O_2} (mm Hg)	Saturation	p_{O_2} (mm Hg)	Saturation	p_{O_2} (mm Hg)	Saturation
0.32	0.0016	17.75	0.2256	49.79	0.8064
0.81	0.0040	18.83	0.2517	53.44	0.8329
1.32	0.0064	19.83	0.2779	57.42	0.8593
1.82	0.0088	20.91	0.3041	62.82	0.8855
2.24	0.0112	22.07	0.3302	69.71	0.9116
2.68	0.0136	23.15	0.3565	80.16	0.9770
3.09	0.0161	24.14	0.3828	100.91	0.9609
3.49	0.0185	25.39	0.4090	140.48	0.9758
3.84	0.0209	26.39	0.4354	163.35	0.9815
4.22	0.0233	27.38	0.4618	194.66	0.9860
4.87	0.0281	28.63	0.4882	233.99	0.9895
5.52	0.0329	29.87	0.5146	277.34	0.9924
6.11	0.0376	31.12	0.5410	328.72	0.9944
7.11	0.0472	32.53	0.5675	381.30	0.9962
8.00	0.0566	33.85	0.5940	436.29	0.9978
8.77	0.0660	35.10	0.6206	492.88	0.9921
9.21	0.0701	36.10	0.6471	524.59	0.9995
11.20	0.0958	38.17	0.6737	555.89	0.9998
12.61	0.1217	39.91	0.7002	589.21	0.9999
14.02	0.1476	41.74	0.7268	622.12	1.0000
15.26	0.1736	43.81	0.7534		
16.59	0.1996	46.30	0.7800		

TABLE III

Adair parameters, whole blood

	$a_1 \times 10^1$	$a_2 \times 10^3$	$a_3 \times 10^3$	$a_4 \times 10^5$
Roughton[a]	0.218 ± 6%	0.912 ± 8%	0.0038 ± 22%	0.247 ± 16%
Roughton[b]	0.237 ± 24%	0.925 ± 20%	0.273 ± 100%	0.253 ± 4%
RW[c]	0.151 ± 10%	0.972 ± 8%	0.170 ± 50%	0.167 ± 2%
MS	0.194	0.645	0.142	0.161
FA	0.151	0.857	0.177	0.142
SC	0.183	0.621	0.162	0.168

[a] From Ref. 1. pH 7.4, p_{CO_2} 40, 37°.
[b] Data of Ref. 1, recalculated according to the procedure of this report.
[c] Errors are for 95% confidence limits.

TABLE IV

Equilibrium constants for successive oxygenation of whole blood

	k_1	k_2	k_3	k_4
Roughton[a]	0.0054 ± 5%	0.028 ± 14%	0.006 ± 30%	2.60 ± 38%
Roughton[b]	0.0059 ± 24%	0.026 ± 44%	0.443 ± 120%	0.037 ± 104%
RW2	0.004 ± 10%	0.043 ± 18%	0.262 ± 58%	0.039 ± 52%

[a] From Ref. 1. pH 7.4, p_{CO_2}, 40, 37°.
[b] Data of Ref. 1, recalculated according to the procedure of this report.

Analysis According to Adair's Equation – The fit of the data to Adair's equation is summarized in Table II and shown in Fig. 5. This procedure as outlined under "Appendix" is rapid, efficient, and highly reproducible. Excellent agreement for the parameters among four subjects was found, but the results differed consistently with the earlier data of Roughton and co-workers (17) (Table III, Fig. 6). The errors in the values of a were determined by systematically varying the value of a_i and then fitting the other 3 a's to the data set. In this way, the residual sum of squares is observed to be a parabolic function of the value of a_i and the 95% confidence limits could be found using the f test. Analysis for one data set is given in Fig. 7.

DISCUSSION

The regulation of the oxygen affinity of hemoglobin within red cells is complex. Much is already known about the qualitative mediation of this regulation, but much remains to be learned about its precise quantitation, about aberrations in pathological states and about possible therapeutic intervention. As a first step toward a quantitative understanding we have attempted to describe the complete curve under conditions which very closely resemble those found *in vivo*. The advantages of our methods over those previously available are the following. (*a*) MetHb and COHb are not present in appreciable amounts, and their quantities are known. (*b*) 2,3-DPG is preserved. (*c*) The entire curve is obtained on the same sample, within a few hours of its collection. (*d*) pH and p_{CO_2} are constant throughout the curve, so that no "corrections" need be made for the Bohr effect. (*e*) Use of the properly calibrated oxygen electrode in the high and low ranges of saturation is more precise than older gasometric methods. (*f*) An analysis of the solubility coefficient (α) can be done on each experiment. (*g*) Analysis of the data according to Adair's scheme is possible.

The curve differs significantly from that reported by Roughton *et al.* (8) (Table III, Fig. 6). The difference can be explained by the fact that the earlier data were obtained before the full importance of 2,3-DPG was appreciated and the older method of deoxygenation required long periods of time during which the blood was held at 37°. Furthermore, the earlier data was "corrected" to pH 7.4 using an assumed Bohr factor. In fact, the Bohr effect is not constant on the entire range of saturation (6, 20, 21). Finally, the earlier data was obtained from blood samples on more than one subject, and the data points were corrected by a factor (observed p_{50}/26.5).

The curves differ in their position on the abscissa by 2.3 mm Hg at 50% saturation, but the difference is less at high saturation, and greater at low saturation. Thus, they differ not only in their position but in their shape, and it is the latter observation for which the Adair analysis is useful. For example, it is known that 2,3-DPG and H^+ exert their influence at low saturation (5), suggesting that either reduced 2,3-DPG or increased intracellular pH (or both) in the older experiments could account for the observed differences.

Furthermore, in our experiments the Bohr protons are titrated as they are released. In methods which employ tonometry of samples with constant CO_2 but differing p_{O_2}, pH and total HCO_3^- will vary with saturation. The effect of pH on the oxygen equilibrium curve is well known, but the effect of HCO_3^- is less well understood (22). Therefore, additional data of the type reported here will be required to fully describe the intracellular effects of H^+, CO_2, HCO_3^-, and 2,3-DPG.

We believe that the principal usefulness in the determination of the Adair parameters is the comparison of the shapes of oxygen equilibrium curves and in quantitatively testing the reproducibility of the curves. The parameters have been used in experiments with pure hemoglobin to calculate the equilibrium constants for the successive oxygenation steps.

These can be calculated as follows (4, 23).

$$k_1 = \left(\frac{1}{4}\right) a_1$$

$$k_2 = \left(\frac{2}{3}\right) \frac{a_2}{a_1}$$

$$k_3 = \left(\frac{3}{2}\right) \frac{a_3}{a_2}$$

$$k_4 = (4) \frac{a_4}{a_3}$$

Thus, the k's will have variances which will be the weighted sum of the co-variances for the a's from which they are calculated, and, except for k_1 will become almost meaningless when the magnitude of the errors is considered (Table III). Nevertheless Table IV summarizes such calculations. The errors are largest in the values of a_2 and a_3 and therefore k_2, k_3, and k_4 will be increasingly less reliable. Therefore, we are not able to attach any physical meaning to the constants of Table III.

The error analysis in Fig. 7 demonstrates that the data can reasonably be described by three parameters, a_1, a_2, and a_4, while the Adair oxygenation scheme (Formula 1) requires four parameters. Therefore, in order to determine the equilibrium constants (k's) from the Adair parameters (a's) data points of even greater number and precision than those in Fig. 6 would be required. We believe that this is extremely unlikely using currently available methods and that other data, perhaps kinetic, would be required.

Acknowledgments – The authors acknowledge with gratitude the many helpful discussions with F. Anderson, A. Nienhuis, A. Minton, and S. Charache, and the expert technical assistance of Ann Baur.

REFERENCES

1. Baldwin, J. M. (1975) *Prog. Biophys. Mol. Biol.* **29**, 225–320
2. Imai, K., Morimoto, H., Kotani, M., Watari, H., Hirata, W., and Kuroda, M. (1970) *Biochim. Biophys. Acta* **200**, 189–196
3. Adair, G. S. (1925) *J. Biol. Chem.* **63**, 529–545
4. Imai, K. (1973) *Biochemistry* **12**, 798–808
5. Tyuma, I., Imai, K., and Shimizu, K. (1973) *Biochemistry* **12**, 1491–1498
6. Imai, K., and Yonetani, T. (1975) *J. Biol. Chem.* **250**, 2227–2231
7. Imai, K., and Yonetani, T. (1975) *J. Biol. Chem.* **250**, 7093–7098

8. Roughton, F. J. W., Deland, E. C., Kernohan, J. C., and Severinghaus, J. W. (1972) in *Oxygen Affinity of Hemoglobin and Red Cell Acid Base Status* (Astrup, P., and Rørth, M., eds) pp. 73–83, Academic Press, New York
9. Rossi-Bernardi, L., Luzzana, M., Samaja, M., Davi, M., DaRiva-Ricci, D., Minoli, J., Seaton, B., and Berger, R. L. (1975) *Clin. Chem.* **21**, 1747–1753
10. Winslow, R. M. (1976) *Proceedings of the Symposium on Molecular and Cellular Aspects of Sickle Cell Disease* Publication No. (NIH) 76-1007, pp. 235–255, United States Department of Health, Education, and Welfare
11. Rossi-Bernardi, L., Perrella, M., Luzzana, M., Samaja, M., and Raffaele, I. (1977) *Clin. Chem.*, in press
12. Nygaard, S. F., and Rørth, M. (1969) *Scand. J. Clin. Lab. Invest.* **24**, 399–403
13. Hahn, C. E. W., Davis, A. H., and Albery, W. J. (1975) *Respir. Physiol.* **25**, 109–133
14. Knott, G. D., and Shrager, R. I. (1972) *Computer Graphics: Proceedings of the SIGGRAPH Computers in Medicine Symposium* Vol. 6, No. 4, pp. 138–151, ACM, SIGGRAPH Notices
15. Shrager, R. I. (1970) *J. Assoc. Computing Machinery* **17**, 446–452
16. Shrager, R. I. (1972) *Comm. Assoc. Computing Machinery* **15**, 41–45
17. Severinghaus, T. W., Roughton, F. J. W., and Bradley, A. F. (1972) in *Oxygen Affinity of Hemoglobin and Red Cell Acid Base Status* (Astrup, P., and Rørth, M., eds) pp. 73–83, Academic Press, New York
18. Seaton, B., and Lloyd, B. B. (1974) *Respir. Physiol.* **20**, 191–207
19. Seaton, B., and Lloyd, B. B. (1974) *Respir. Physiol.* **20**, 209–230
20. Tyuma, I., Kamigawara, Y., and Imai, K. (1973) *Biochim. Biophys. Acta* **310**, 317–320
21. Hlastala, M. P., and Woodson, R. D. (1975) *J. Appl. Physiol.* **38**, 1126–1131
22. Kreuger, F., Roughton, F. J. W., Rossi-Bernardi, L., and Kernohan, J. C. (1972) in *Oxygen Affinity of Hemoglobin and Red Cell Acid Base States* (Astrup, P., and Rørth, M., eds) pp. 208–215, Academic Press, New York
23. Deal, W. J. (1973) *Biopolymers* **12**, 2057–2073

Appendix

Analysis of the Data According to Adair's Scheme

The principal difficulty in fitting data to the Adair equation is in obtaining the initial estimates of the a's.

Consider the problem of fitting a formula f(p,a) to some data y(p) where p is the independent variable, and a is a vector of parameters to be found. The vectors y and f are related by:

$$y_i(p) = f_i(p,a) + \epsilon_i \tag{1}$$

where ϵ_i is presumed to be the error in y_i, that error being uncorrelated from observation to observation, and having finite variance. Now suppose the formula f is difficult to work with, perhaps because it is nonlinear in the parameters a. It is decided that a transformed problem will be used. Let g be that transformation, a differentiable function of one variable:

$$g(y_i) = g(f_i + \epsilon_i) = g(f_i) + \gamma_i \tag{2}$$

where γ is the error one gets in the transformed fit of g(f) to g(y). If ϵ is sufficiently small then one can use the approximation:

$$\gamma_i = \epsilon_i \, dg(f_i)/df_i \tag{3}$$

or, since f is not known in advance:

$$\gamma_i = \epsilon_i \, dg(y_i)/dy_i \tag{4}$$

Prior information about errors like ϵ in (1) or γ in (2) is important, because minimum variance estimates of the parameters a are achieved when the sum of squares to be minimized in (1) is:

$$\Sigma w_i (y_i - f_i)^2$$

where

$$w_i = 1/\mathrm{var}(y_i) = 1/\mathrm{var}(\epsilon) \tag{5}$$

or in (2):

$$\Sigma \tilde{w}_i [g(y_i) - g(f_i)]^2$$

where

$$\tilde{w}_i = 1/\mathrm{var}\,[g(y_i)] = 1/[(\tfrac{\partial g}{\partial y_i})^2 \mathrm{var}(y_i)] = w_i/(\tfrac{\partial g}{\partial y_i})^2 \tag{6}$$

Therefore, when using the easier formula (2), the weights (5) must be corrected by certain factors (6), but it is not always obvious as to what those factors should be, because they involve $\sigma_{\epsilon i}$ or f which are not yet known.

The Adair equation can be rewritten:

$$y_i = f_i = p_i v'(p_i)/4v(p_i) \tag{7}$$

where

$$v(p_i) = 1 + a_1 p_i + a_2 p_i^2 + a_3 p_i^3 + a_4 p_i^4$$

$$v'(p_i) = dv(p_i)/dp_i = a_1 + 2a_2 p_i + 3\,a_3 p_i^2 + 4a_4 p^3$$

This formula (7) is nonlinear in the a's, which are the parameters to be found. Therefore, the solution to the least squares problem will be iterative, requiring good first estimates of the a's to insure rapid convergence to the proper solution. To generate these estimates, one may multiply (7) by $v(p_i)$ and rearrange terms to get:

$$y_i = a_1 p_i (\tfrac{1}{4} - y_i) + a_2 p^2 (\tfrac{1}{2} - y_i) + a_3 p^3 (\tfrac{3}{4} - y_i) + a_4 p^4 (1 - y_i) \tag{8}$$

which is now linear in the a's and can be solved in one step by ordinary least squares, provided there are reasonable weights.

The method used by Roughton, et al (1), also used by Imai (5), uses only four points, and solves (8) exactly. Consequently, their estimates of the a's are subject to the error in those few points. The method proposed here will estimate the initial a's with considerably smaller variance because the entire set of points is used, resulting in fewer iterations in the nonlinear curve-fitting phase. Using the technique suggested in (6), we note that:

$$f(y_i) = y_i \, v(p_i)$$

and

$$\partial g/\partial y_i = v(p_i) \tag{9}$$

Therefore

$$\tilde{w}_i = w_i/v^2(p_i)$$

The weights for (8) are much different from those for (7), because in (8) the y's, with their errors, appear on the right side where they are multiplied by large powers of P. Hence the discrepancy between the left and right sides in (8) will be exaggerated for large P.

In order for (9) to be useful, an approximation to $v(P_i)$ must be generated, because the a's are not yet known. To this end, formula (7) may be rewritten

$$\frac{4y_i}{p_i} = \frac{d}{dp_i} \ln(v(p_i)) \tag{10}$$

Assuming equality, one multiplies by dp_i and integrates:

$$4 \int_0^P \frac{y}{u}\, du = \ln(v) \tag{11}$$

or

$$v(p_i) = e^{4 \int_0^{p_i} \frac{y}{u}\, du} \tag{12}$$

or

$$\tilde{w}_i = c\, e^{-8 \int_0^{p_i} \frac{y}{u}\, du} \tag{13}$$

the integral in (13 can be approximated directly from the data by the trapezoidal rule

$$\int_0^{p_i} \frac{y}{u}\, du \approx \tfrac{1}{2} [y_i + \sum_{j=2}^{i} (\frac{y_{j-1}}{p_{j-1}} + \frac{y_j}{p_j})(p_j - p_{j-1})]. \tag{14}$$

where the data have been sorted so that

$$0 < p_1 < p_2 \ldots < p_n$$

The complete fitting procedure for the Adair equation is:

1. Evaluate the integral in (14)
2. Compute the weights in (13)
3. Fit using formula (8) and weights (13) to generate first estimates of the a's.
4. Refine the a's by a fit using the Adair equation with weights (5).

The fourth step is necessary because the weights in (13) are only approximate, and also because saturation in the Adair equation, unlike formula (8), is not subject to point for point fluctuations in y, i.e., the right side of the Adair equation closely approximates a theoretical curve, whereas the right side of formula (8) does not.

In theory, Hb would not be expected to be 100% saturated at oxygen tensions which are practically achievable. The fit of the data to the Adair scheme can therefore be improved somewhat by determining the theoretical saturation at the highest pO_2 using the estimated a's for step (4) above. This saturation can then be used to obtain a second set of saturations which can be used for a final refinement of the a's.